Charge transport mechanisms of graphene/semiconductor Schottky barriers: A theoretical and experimental study

Haijian Zhong,[1] Ke Xu,[1,2,a)] Zhenghui Liu,[1] Gengzhao Xu,[1] Lin Shi,[1] Yingmin Fan,[1] Jianfeng Wang,[1,2] Guoqiang Ren,[1,2] and Hui Yang[1]
[1]*Suzhou Institute of Nano-Tech and Nano-Bionics, CAS, Suzhou 215123, People's Republic of China*
[2]*Suzhou Nanowin Science and Technology Co., Ltd., Suzhou 215123, People's Republic of China*

(Received 21 August 2013; accepted 12 December 2013; published online 3 January 2014)

Graphene has been proposed as a material for semiconductor electronic and optoelectronic devices. Understanding the charge transport mechanisms of graphene/semiconductor Schottky barriers will be crucial for future applications. Here, we report a theoretical model to describe the transport mechanisms at the interface of graphene and semiconductors based on conventional semiconductor Schottky theory and a floating Fermi level of graphene. The contact barrier heights can be estimated through this model and be close to the values obtained from the experiments, which are lower than those of the metal/semiconductor contacts. A detailed analysis reveals that the barrier heights are as the function of the interface separations and dielectric constants, and are influenced by the interfacial states of semiconductors. Our calculations show how this behavior of lowering barrier heights arises from the Fermi level shift of graphene induced by the charge transfer owing to the unique linear electronic structure. © *2014 AIP Publishing LLC*. [http://dx.doi.org/10.1063/1.4859500]

I. INTRODUCTION

Graphene is a single layer two-dimensional carbon sheet with the hexagonal lattice. Owing to its distinctive band structure, graphene has attracted an increasing considerable interest in the application in electronic and optoelectronic devices over recent years. Graphene/semiconductor junctions are of great importance to the fabrication of high-performance graphene electronic and optoelectronic devices.[1–8] Understanding the transport mechanisms of graphene on semiconductors is crucial to improving the performance of graphene devices.

Various performances have been investigated for graphene/semiconductor devices, including GaN and organic light-emitting diodes (LEDs)[4–6] and silicon and polymer-based photovoltaic cells.[8–10] Therefore, interactions of graphene/semiconductor have attracted increased attention recently.[11–14] Barrier heights have been measured between few-layer or a mix of single-layer, bi-layer, and few-layer graphene and a semiconductor.[2,3,8,15] In these applications, graphene/semiconductor junctions have been usually treated as traditional Schottky diodes with an invariant Fermi level of graphene just like metal. However, even in few-layer graphene, the Fermi level can be shifted by the charge carrier transfer,[16,17] which subsequently affects barrier heights. For pristine single-layer graphene (SLG), the Fermi level is aligned with Dirac points and the density of states (DOS) vanishes exactly at the Fermi energy.[18] It can be calculated that a transfer of 0.01 electrons per unit cell would shift the Fermi level by 0.47 eV.[19] This transport mechanism is quite different from that of conventional metals. The high-resistance barriers in conventional Schottky devices are mainly derived from the Fermi level differences and the associated charge transfer between metals and semiconductors.[20] The charge transfer can barely vary the Fermi level because of their high DOS at the Fermi energy. Therefore, despite some experimental progress in graphene devices, a systematic study estimating the interaction effects of graphene/semiconductor with a theoretical model, as well as their interfacial states and the resulting changes of the barrier height, is lacking.

The objective of this study is to fully understand the transport mechanisms of graphene/semiconductor junctions using a physical modeling based on the traditional Schottky theory and the unique energy structure in graphene. The theoretical analysis indicates that the graphene Fermi level shifts with the charge transfer from/to semiconductors resulting in the decrease of the Schottky barrier heights. The Schottky barrier heights can also be quantitatively deduced for the graphene/semiconductor contacts from our model. The effects of the carrier density of semiconductors, interfacial states, and dielectric constants on Schottky barrier heights have also been taken into account. The verified experiments were performed using conductive atomic force microscopy (CAFM), in which the experimental barrier heights match the theoretical calculations well proving the rationality of the model.

This paper is organized as follows: The theoretical models for depicting the transport mechanism between graphene and semiconductors are introduced in Sec. II. The considerations of the ideal condition and interfacial states are illustrated, respectively. In Sec. III, the experimental methods are described detailedly, including the preparation of the samples and measurement setup. Compared with experimental results, the key factors influencing the transport properties are discussed with a fully numerical calculation in Sec. IV. The verified experiments of exfoliated graphene/n-SiC contacts are also demonstrated. The final section is devoted to some concluding remarks.

a)Electronic mail: kxu2006@sinano.ac.cn

II. THEORETICAL MODELS

As we know, the charge carrier transfer exists in the metal-semiconductor interfaces and the Fermi level changes only in the semiconductor as demonstrated in Figs. 1(a) and 1(b). In virtue of the different electronic property of graphene mentioned above, we propose that graphene has a potential ability to form low barrier-height contacts with both *n*-type and *p*-type semiconductors. As illustrated in Figs. 1(c) and 1(d), the charge carrier transport between graphene and semiconductor substrates will break the symmetry of the electron and hole concentration in the graphene. When the electrons transfer from the bulk *n*-type semiconductor into the graphene, the graphene's Fermi level will be raised up from the Dirac points towards that of the *n*-type semiconductor, and the barrier heights will be reduced. Applying the same reasoning to the contact between graphene and a *p*-type semiconductor, the hole transfer from the *p*-type semiconductor will positively charge the graphene and decrease its Fermi level, which also results in a reduction of the barrier heights.

To quantitatively estimate the barrier heights and Fermi level shift of the graphene and investigate the transport mechanisms, we presented a model based upon traditional Schottky barrier theory and considered the case of the gallium nitride (GaN) semiconductor.

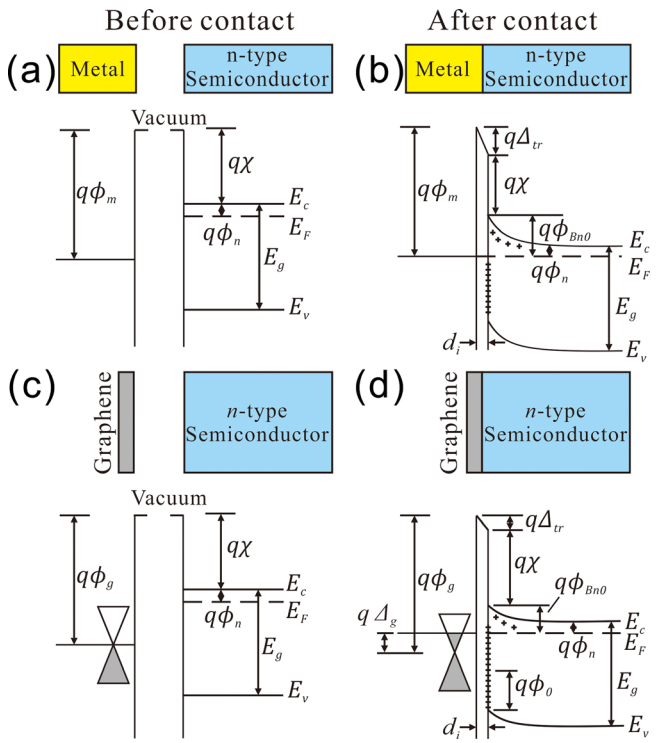

FIG. 1. (a) Metal and *n*-type semiconductor in separated systems. (b) Metal and *n*-type semiconductor connected into one system in which a Schottky barrier is formed. (c) Graphene and *n*-type semiconductor in separated systems. (d) Graphene and *n*-type semiconductor connected into one system in which the effects of interfacial states is also taken into account. Definition of symbols: ϕ_m and ϕ_g are the work functions of metal and neutral graphene, respectively. χ is the electron affinity of the semiconductor and E_g is band gap. $q\phi_n$ is the energy difference between the bottom energy of the conduction band E_c and the Fermi level E_F. ϕ_{Bn0} is the barrier height. ϕ_0 is the neutral level of the interfacial states above valance band E_v. Δ_g is the work function shift of graphene relative to the Dirac points. Δ_{tr} is the potential drop on the interfacial gap d_i between graphene.

A. An ideal theoretical model

In ideal condition, there are no surface states and other anomalies in semiconductor surface. Fig. 1(c) shows the band structure relations of a higher work-function graphene and an *n*-type GaN (*n*-GaN), which are not in contact and are in separate systems. The conduction band and valance band of the *n*-GaN keeps flat. When graphene and *n*-GaN are in contact, as shown in Fig. 1(d), charge carriers will transfer from the *n*-GaN to the graphene and form a single system at the request of thermal equilibrium. Because of the linear band dispersion of graphene different from metal, the Fermi level of graphene will shift upwards, meanwhile the Fermi level in the semiconductor is lowered. The Fermi levels will finally line up on both sides.

As is known to all, that the density of states of the graphene is given by

$$\rho(E) = \left[\frac{2}{\pi}\frac{|E|}{(\hbar v_F)^2}\right] = D_0|E|. \tag{1}$$

The equation relating charge Q_G transferred into the graphene to Fermi level shift Δ_g is given by

$$Q_G = -q \cdot \mathrm{sign}(\Delta_g)\int_0^{q\Delta_g}\rho(E)dE = -\frac{1}{2}\mathrm{sign}(\Delta_g)\cdot q^3 D_0 {\Delta_g}^2. \tag{2}$$

And Fermi level shift Δ_g of the graphene can be obtained

$$\Delta_g = -\mathrm{sign}(Q_G)\sqrt{\frac{2}{q^3}\frac{|Q_G|}{D_0}}. \tag{3}$$

The potential difference Δ_{tr} across the interfacial layer can be obtained by applying Gauss' law to charge Q_G transferred into the graphene

$$\Delta_{tr} = -\frac{Q_G \cdot d_i}{\varepsilon_0 \varepsilon_i}, \tag{4}$$

where ε_0 and ε_i are the dielectric constant of vacuum and the interface between graphene and GaN.

For contacts between graphene and *n*-GaN in thermal equilibrium condition, the space charge Q_s in the depletion layer is given by

$$Q_s = \mathrm{sign}\left(\phi_{Bn0} - \phi_n - \frac{kT}{q}\right)\sqrt{2q\varepsilon_r\varepsilon_0 n\left|\phi_{Bn0} - \phi_n - \frac{kT}{q}\right|}, \tag{5}$$

where ε_r, n, and ϕ_n are the relative dielectric constant of GaN, the carrier density, and the energy difference between the bottom energy of conduction band E_c and the Fermi level E_F.

Based on the charge conservation law, the net charge is zero,

$$Q_s + Q_G = 0. \tag{6}$$

From Eqs. (2), (5), and (6), Fermi level shift Δ_g is determined as a function of barrier height ϕ_{Bn0}.

Another relation about Fermi level shift Δ_g and barrier height ϕ_{Bn0} can also be acquired by inspection of the energy-band diagram of Fig. 1(d)

$$\phi_g - \Delta_g = \Delta_{tr} + \chi + \phi_{Bn0}. \tag{7}$$

Therefore, Fermi level shift Δ_g and barrier height ϕ_{Bn0} can be obtained by solving the two simultaneous Eqs. (6) and (7).

The model above is also suitable for contacts between graphene and *p*-type GaN (*p*-GaN). There are two differences from *n*-type case, in which the space charge Q_s is written as

$$Q_s = \mathrm{sign}\left(\phi_{Bp0} - \phi_p - \frac{kT}{q}\right)\sqrt{2q\varepsilon_r\varepsilon_0 n\left|\phi_{Bp0} - \phi_p - \frac{kT}{q}\right|}, \tag{8}$$

and the equation from the energy-band diagram is given by

$$\phi_g + \Delta_g + \Delta_{tr} = \frac{E_g}{q} - \phi_{Bp0} + \chi. \tag{9}$$

B. A theoretical model considering interfacial states

Interfacial states in semiconductors have been frequently reported to influence the contact properties and performance of electronic and optoelectronic devices. The interfacial states would have to be donors to contribute additional free electrons to the graphene in contact with semiconductors. These states may be caused by dangling bonds or vacancies or they may be ionic in the form of a substitutional donor species such as oxygen. All of these possible sources of mobile carriers may contribute in some proportion to the charge transfer in an actual contact system between graphene and semiconductors.

As we know, the interfacial states in metal-semiconductor contacts can be simply described by neutral level ϕ_0 and DOS D_{it}. ϕ_0 is the energy level about E_V at semiconductor surface, which is negatively charged when $E_F > q\phi_0$ and is positively charged when $E_F < q\phi_0$. The DOS of interfacial states for semiconductors is usually believed to be invariant when semiconductors are in contact with different metals, which was verified by performing the first-principles calculations to investigate the partial density of states (PDOS) of GaN for Au, Pt atoms and graphene absorption on c-plane GaN surfaces based on the density functional theory (DFT), respectively, using the Vienna *ab initio* simulation package (VASP) code. As shown in Fig. 2, the sum of the PDOS of s-, p-, and d-orbitals of Ga atoms on the GaN surfaces at GaN Fermi energy alters little when Au, Pt atoms and graphene are absorbed on the GaN surfaces, respectively. D_{it} and ϕ_0 can be calculated because they are the properties of the semiconductor surface and are independent of the contact material. Assuming that the DOS of

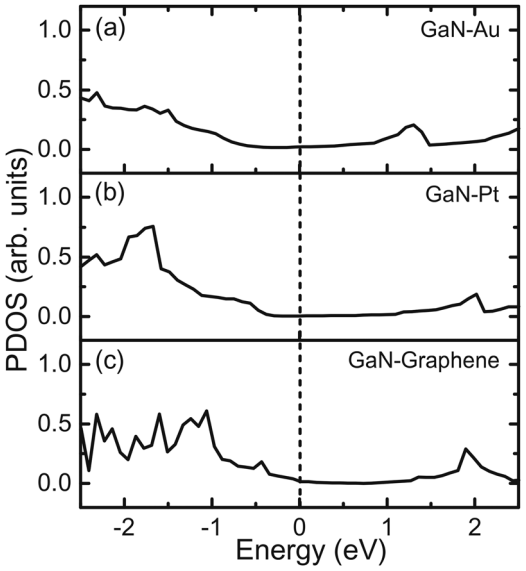

FIG. 2. The DFT calculation results of the PDOS of Ga atoms on the GaN surfaces for the clean GaN surfaces and physical absorption of Au atoms (a), Pt atoms (b), and graphene on the GaN surfaces (c).

interfacial states is D_{it} states/(cm^2 eV), the interfacial charge density Q_i on *n*-GaN surface is given by[20]

$$Q_i = -qD_{it}\cdot(E_g - q\phi_0 - q\phi_{Bn0}). \tag{10}$$

For metal contact to *n*-GaN, the alignment of Fermi level gives an equation[20]

$$\phi_m - \chi - \phi_{Bn0} = \sqrt{\frac{2q\varepsilon_r\varepsilon_0 n d_i^2}{\varepsilon_i^2\varepsilon_0^2}\left|\phi_{Bn0} - \phi_n - \frac{kT}{q}\right|} - \frac{qD_{it}d_i}{\varepsilon_i\varepsilon_0}(E_g - q\phi_0 - q\phi_{Bn0}). \tag{11}$$

With the two known different metals contact to *n*-GaN surfaces, the barrier heights between metal and *n*-GaN can be obtained from the current-voltage (*I-V*) curves as measured in the experiments, respectively. An equations group can be achieved and D_{it} and ϕ_0 for *n*-GaN can be solved.

For the case of graphene contact to *n*-GaN, the balance of charge in the graphene, the interface, and the depletion region of the semiconductor gives

$$Q_G = -(Q_s + Q_i). \tag{12}$$

Using Eqs. (5) and (10) to substitute for Q_s and Q_i in Eq. (12), we can express Q_G as a function of ϕ_{Bn0}

$$Q_G(\phi_{Bn0}) = qD_{it}\cdot\left(E_g - q\phi_0 - q\phi_{Bn0}\right) - \mathrm{sign}\left(\phi_{Bn0} - \phi_n - \frac{kT}{q}\right)\times\sqrt{2q\varepsilon_r\varepsilon_0 n\left|\phi_{Bn0} - \phi_n - \frac{kT}{q}\right|}. \tag{13}$$

Using Eqs. (3), (4), and (13) to substitute for Δ_g, Δ_{tr}, and Q_G in Eq. (7), respectively, a function is obtained as

$$V(\phi_{Bn0}) = -\text{sign}[Q_G(\phi_{Bn0})]\sqrt{\frac{2}{q^3}\frac{|Q_G(\phi_{Bn0})|}{D_0}} - \frac{Q_G(\phi_{Bn0})\cdot d_i}{\varepsilon_i\varepsilon_0} + \phi_{Bn0} - (\phi_g - \chi). \quad (14)$$

When $V(\phi_{Bn0})$ touches zero, the barrier height ϕ_{Bn0} can be solved numerically by plotting $V(\phi_{Bn0})$ versus ϕ_{Bn0}.

For the p-type semiconductors, the interfacial states D_{it} and neutral level ϕ_0 can also be figured out using the methods similar to the n-type semiconductors. According to the band alignment and the thermal equilibrium condition, an equation for the metal/p-GaN junctions is given as follows:

$$\phi_m + \phi_{Bp0} - E_g - \chi = \sqrt{\frac{2q\varepsilon_r\varepsilon_0 p{d_i}^2}{{\varepsilon_i}^2{\varepsilon_0}^2}\left|\phi_{Bp0} - \phi_p - \frac{kT}{q}\right|} - \frac{qD_{it}d_i}{\varepsilon_i\varepsilon_0}(q\phi_0 - q\phi_{Bp0}). \quad (15)$$

When graphene is in contact with the p-GaN, as shown in Fig. 3, the interfacial charge density Q_i on p-GaN surface is given by

$$Q_i = qD_{it}\cdot(q\phi_0 - q\phi_{Bp0}). \quad (16)$$

Using Eqs. (8) and (16) to substitute for Q_s and Q_i in Eq. (12), we can express Q_G as a function of ϕ_{Bp0}

$$Q_G(\phi_{Bp0}) = -qD_{it}\cdot(q\phi_0 - q\phi_{Bp0}) + \text{sign}\left(\phi_{Bp0} - \phi_p - \frac{kT}{q}\right) \times \sqrt{2q\varepsilon_r\varepsilon_0 n\left|\phi_{Bp0} - \phi_p - \frac{kT}{q}\right|}. \quad (17)$$

Using Eqs. (3), (4), and (17) to substitute for Δ_g, Δ_{tr}, and Q_G in Eq. (9), respectively, a function is obtained as

$$V(\phi_{Bp0}) = \text{sign}[Q_G(\phi_{Bp0})]\sqrt{\frac{2}{q^3}\frac{|Q_G(\phi_{Bp0})|}{D_0}} + \frac{Q_G(\phi_{Bp0})\cdot d_i}{\varepsilon_0\varepsilon_i} + \frac{E_g}{q} - \phi_{Bp0} + \chi - \phi_g. \quad (18)$$

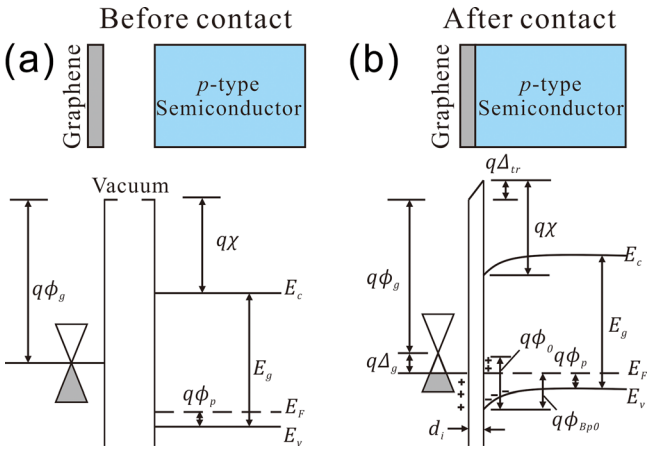

FIG. 3. (a) Graphene and p-type semiconductor in separated systems. (b) Graphene and p-type semiconductor connected into one system with the interfacial states.

The barrier height ϕ_{Bp0} can be solved numerically by plotting $V(\phi_{Bp0})$ versus ϕ_{Bp0} as the value of $V(\phi_{Bp0})$ is zero.

III. EXPERIMENTAL DETAILS

In order to verify the reliability and veracity of the barrier model, the barrier heights of graphene and GaN were measured using C-AFM method. SLG films were prepared by micro-mechanical exfoliation of Kish graphite.[21] The exfoliated graphene films were transferred by the scotch-tape method onto native n-type and Mg-doped p-type GaN substrates for comparative studies.[22,23] The number of graphene layers was identified using Raman spectra with a 632.8 nm wavelength laser. Both n-GaN and p-GaN films were grown on (0001) sapphire by the metal-organic chemical vapor deposition (MOCVD) method. Their carrier density characterized by Hall measurements were $5.0\times10^{18}\,\text{cm}^{-3}$ and $4.5\times10^{17}\,\text{cm}^{-3}$, respectively. Fig. 4 shows the schematic setup employed for our experiments. The ohmic electrode of indium for the n-GaN was fabricated by thermal welding with electric breakdown between them. The as-deposited Ni(10 nm)/Au(50 nm) ohmic contact for p-GaN was achieved by air annealing in 500 °C for 5 min. Both ohmic contacts for n- and p-GaN prepared at surface corners were ensured by the I-V measurements using probe station (PM8 from SUSS Microtech AG, Germany). The local transport properties of graphene in contact with GaN samples were studied by C-AFM (NT-MDT NTEGRA Spectra) in contact mode with a metal-coated tip as a grounded electrode for the current collection. The C-AFM measurements were performed by Au-coated tip (ATEC-FMAu from Nanosensors Company) and Pt-coated tip (ANSCM-Pt from Appnano Company), respectively. The topography of samples was acquired first in non-contact mode with resonant frequency of about 60–80 KHz. Then, the I-V curves were measured at a chosen position in contact mode with a constant contact force of about 500 nN.

IV. RESULTS AND DISCUSSION

Figs. 5(a) and 5(e) show the topography of an isolated graphene on an n-GaN and a p-GaN substrate, respectively. Raman spectra as shown in Figs. 5(c) and 5(g) confirm the graphene sheets to be a single layer.[24] Unlike previous studies of mechanically cleaved SLG on smooth substrates,[23,25,26]

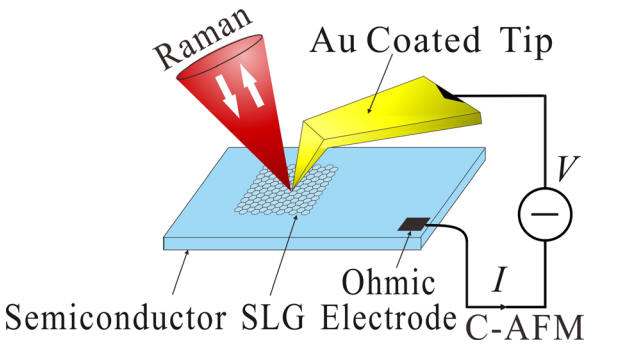

FIG. 4. Schematics for C-AFM measurements with a metal-coated tip showing the tip in contact mode with biased semiconductor layer and Raman measurements with a 632.8 nm wavelength laser.

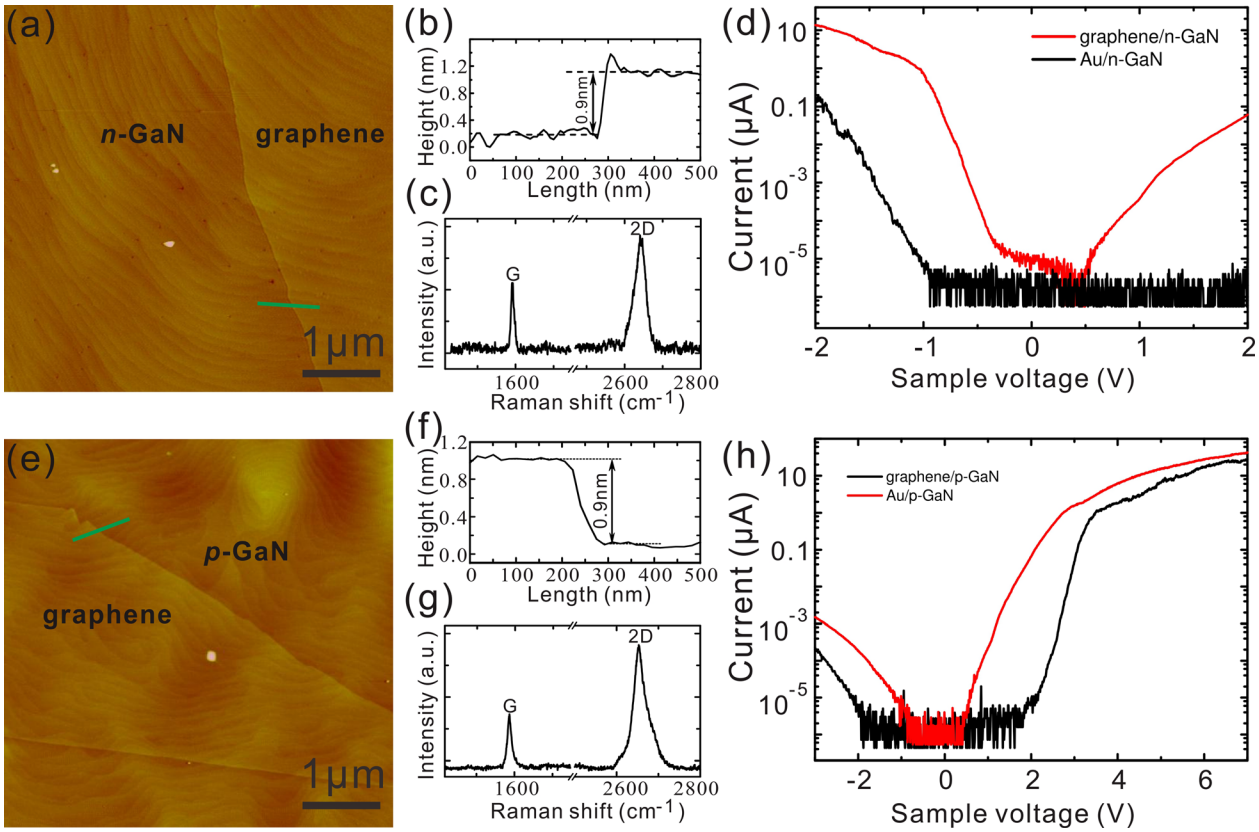

FIG. 5. AFM images of an isolated SLG sheet on an *n*-GaN (a) and a *p*-GaN (e) substrate. The green lines across the boundary between graphene and GaN indicate the profile for the heights shown in (b) and (f) at approximately 0.9 nm both for the *n*-GaN and the *p*-GaN samples. Inset: Diagram of integrated C-AFM and Raman measurements with an Au-coated tip. (c) and (g) Raman spectra (632.8 nm laser wavelength) obtained from the graphene in (a) and (e). (d) and (h) Local *I-V* curves, acquired from bare *n*- and *p*-GaN (black lines) surfaces and graphene sheets (red lines), respectively.

AFM line profiles should be on the same GaN terrace and should cross the boundary between graphene and GaN to minimize the effects of corrugations from GaN terraces as shown in Figs. 5(b) and 5(f). The heights of the graphene sheets have been determined to be approximately 0.9 ± 0.2 nm for both the *n*-GaN and *p*-GaN samples, respectively. These values are approximate to the SLG reported values of about 1.0 nm on other substrates.[23,24,27]

Typical *I-V* curves for *n*- and *p*-GaN are plotted in Figs. 5(d) and 5(h), respectively, using the C-AFM method by the Au-coated AFM tip. The black symbol indicates the Au-coated tip on *n*-GaN and the red symbol is for graphene. An obvious rectifying behavior similar to a Schottky barrier is observed. The barrier heights at the Au-coated tip/GaN and the Au-coated tip/graphene/GaN interfaces can be obtained by the least squares method using the expression.[20]

$$I = AA^{*}T^{2}\exp\left(-\frac{q\phi_B}{kT}\right)\left[\exp\left(\frac{qV}{\eta kT}\right) - 1\right], \qquad (19)$$

where I and V are the device current and applied voltage, respectively; A, A^{*}, T, q, k, and η are the Schottky contact area, the Richardson constant ($26.4\,\mathrm{A\,cm^{-2}\,K^{-2}}$ for *n*-GaN and $96.1\,\mathrm{A\,cm^{-2}\,K^{-2}}$ for *p*-GaN), room temperature (300 K), electron charge, Boltzmann constant, and the ideality factor, respectively. For the Au/GaN junction, the Schottky contact radius, r, can be calculated using the Hertz model, which is described by[28]

$$r = \left[\frac{3}{4}FR\left(\frac{1-\nu_1{}^2}{Y_1} + \frac{1-\nu_2{}^2}{Y_2}\right)\right]^{\frac{1}{3}}, \qquad (20)$$

where F, R, Y, and ν are the load, the Au-coated tip radius, the Young's modulus, and the Poisson's ratio, respectively. With $F = 450$ nN, $R = 80$ nm, $Y_1 = 78$ GPa and $\nu_1 = 0.44$ for Au, $Y_2 = 295$ GPa and $\nu_2 = 0.25$ for GaN,[29] and r is calculated to be about 7 nm with the Schottky contact area around 154 $\mathrm{nm^2}$. When the Au-coated tip is located on the graphene/GaN surface, because of only a monatomic layer for the SLG, the surface mechanical properties will be dominated by the GaN substrate.[30] Therefore, we assume that the contact area for the Au-coated tip on the graphene/GaN surface equates approximately to the calculated contact area of Au-coated tip on GaN surface with the value of 154 $\mathrm{nm^2}$.

The barrier heights of the tip/*n*-GaN and tip/graphene/*n*-GaN systems can be figured out statistically from the *I-V* data to be 0.53 ± 0.05 V and 0.33 ± 0.02 V, respectively, repeated on 9 *I-V* curves. Similarly, the barrier heights of the tip/*p*-GaN and tip/graphene/*p*-GaN systems can also be acquired through the typical *I-V* curves in Fig. 5(h). The statistical barrier height was 0.86 ± 0.23 V on bare *p*-GaN and was reduced to 0.40 ± 0.05 V on the graphene-covered surface.

The barrier heights of graphene/*n*-GaN and graphene/*p*-GaN junctions can also be obtained through our theoretical model. The required parameters for calculations are listed as

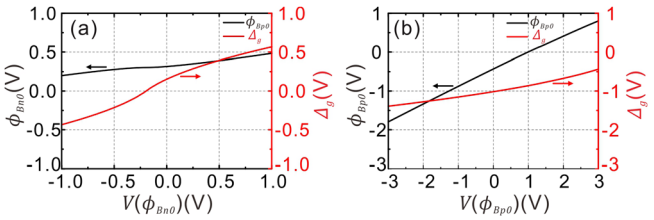

FIG. 6. The calculation results of the barrier height and the Fermi level shift using the theoretical model considering the interfacial states for graphene/*n*-GaN junction (a) and graphene/*p*-GaN junction (b).

follows. The work function of the neutral graphene, ϕ_g, is 4.6 V.[31,32] The relative dielectric constant of the interfacial surface, ε_i, is 5.7 (the median value of the vacuum (1.0) and the GaN (10.4)). The affinity of GaN, χ, is 4.1 V. The value of d_i for graphene/*n*-GaN and graphene/*p*-GaN can be estimated as about 0.6 nm by subtracting the thickness of the SLG (0.34 nm) from the experimental step heights of the graphene measured by AFM (both 0.9 nm) as shown in Figs. 5(b) and 5(f). For the *n*-GaN sample with a carrier density of $5.0 \times 10^{18}\,\mathrm{cm}^{-3}$, the barrier heights measured on the bare *n*-GaN surface by Au- and Pt-coated tips are 0.53 ± 0.05 V and 0.71 ± 0.04 V, respectively. The values of D_{it} and neutral level ϕ_0 were calculated to be 1.25×10^{14} $\mathrm{eV}^{-1}\,\mathrm{cm}^{-2}$ and 3.06 V, respectively. When these parameters are introduced into our model, the barrier height of graphene/*n*-GaN junction can be estimated as 0.32 V and the Fermi level shift of graphene Δ_g is 0.15 V as shown in Fig. 6(a). For the *p*-GaN samples with a carrier density of $4.5 \times 10^{17}\,\mathrm{cm}^{-3}$, the barrier heights measured on the bare *p*-GaN surface by Au- and Pt-coated tips are -0.86 ± 0.23 V and -0.55 ± 0.06 V, respectively. The values of D_{it} and neutral level ϕ_0 were calculated to be $4.75 \times 10^{13}\,\mathrm{eV}^{-1}\,\mathrm{cm}^{-2}$ and -1.13 V, respectively. The barrier height of graphene/*p*-GaN junction can be estimated at about -0.43 V and the Fermi level shift of graphene Δ_g is -1.02 V as shown in Fig. 6(b). The experimental values of the barrier heights are close to the results from the calculation for both *n*-type and *p*-type GaN. The calculated barrier heights and Fermi level shifts for graphene/GaN junctions are listed in Table I considering the conditions both with and without the interfacial states, which shows that the calculated results without the interfacial states deviate from the experimental results.

Noting the large band gap width of 3.4 eV of GaN, the above experimental and theoretical results verified that graphene can adapt its Fermi level to either type of GaN when they are in contact and has a lower barrier height.

TABLE I. The calculated and experimental results of the barrier heights and Fermi level shift without D_{it} and with D_{it}.

	Calculations				
	Without D_{it}		With D_{it}		Experiments
Junctions	ϕ_{Bn0}/ϕ_{Bp0} (V)	Δ_g (V)	ϕ_{Bn0}/ϕ_{Bp0} (V)	Δ_g (V)	ϕ_{Bn0}/ϕ_{Bp0} (V)
SLG/*n*-GaN	0.10	0.18	0.32	0.15	0.33 ± 0.02
SLG/*p*-GaN	-2.60	-0.23	-0.43	-1.02	-0.40 ± 0.05

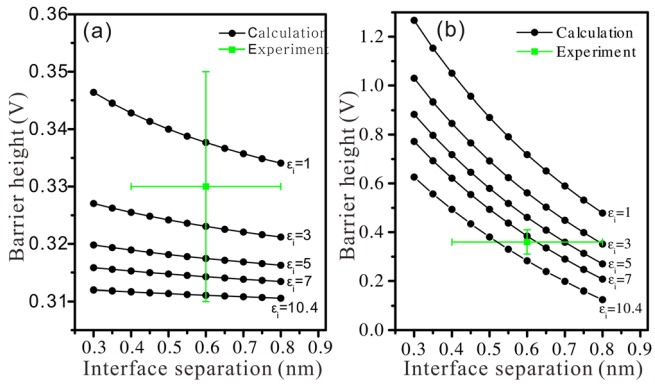

FIG. 7. Effects of interface separations (d_i) and dielectric constants (ε_i) on barrier heights. (a) Calculated barrier heights vs. interface separation for different ε_i, in the region between the graphene and the *n*-GaN (black lines). The experimental values are indicated by green dots. (b) Calculated and experimental results for the graphene contact to the *p*-GaN. The error bars reflect the variance of the repeated measurements.

In our theoretical model, four key factors influence the calculated barrier heights: the interface separation (d_i), the relative dielectric constant in the interface gap (ε_i), the carrier density in the semiconductor (n), and the DOS of interfacial states (D_{it}). These will be further discussed below.

Among the four parameters, ε_i and d_i are difficult to be determined by experiments usually. Using our theoretical model, we calculated the dependence of the barrier height on d_i with different ε_i between the graphene and the *n*- and *p*-GaN. As shown in Fig. 7, when the interface separations increase from 0.3 to 0.8 nm for graphene/*n*-GaN and graphene/*p*-GaN, the barrier heights will decrease due to the greater potential drops on the gap. It should be noted that a gap with even larger separations cannot be assumed to be transparent for carriers, making our model inappropriate. The effective dielectric constant value can be between the vacuum and the GaN. With a larger ε_i, the calculated barrier heights decrease. According to this calculation, the values of ε_i and d_i can be evaluated easily. For example, in our previous experimental results, the values of d_i for graphene/*n*-GaN and graphene/*p*-GaN were both measured to be about 0.6 nm from the AFM images. Hence, the effective dielectric constant ε_i can be estimated to be about 2 and 7, for the graphene on *n*-GaN and *p*-GaN surfaces, respectively, from Fig. 7.

The effects of two other parameters, *n* and D_{it}, were studied experimentally by transferring exfoliated graphene sheets on *n*-GaN surfaces with different carrier densities, respectively. The experimental and calculated results are listed in Table II. In our model, regardless of the interfacial states ($D_{it} \to 0$), the barrier heights will be solely determined by the space charge density. They were found to decrease by 0.26 V with the carrier densities increasing by three orders of magnitude. If D_{it} is considered, the charge transfer from interfacial states also contributes to the barrier heights. The calculated barrier heights will decrease by only about 0.07 V with carrier densities increasing by three orders of magnitude. The experimental results show a change in barrier heights of only about 0.01 V with different carrier densities. The results for *n*-GaN show that the barrier heights were slightly influenced by the carrier density *n*. The proper estimate of the barrier heights

TABLE II. The effects of the carrier density (n) and the DOS of interfacial states (D_{it}) of n-GaN on the experimental barrier heights (ϕ_{Bn0}) and the calculated barrier heights.

				Calculations		Experiments
Junctions	n (cm^{-3})	D_{it} ($cm^{-2}\cdot eV^{-1}$)	ϕ_0 (V)	ϕ_{Bn0} without D_{it} (V)	ϕ_{Bn0} with D_{it} (V)	ϕ_{Bn0} (V)
Gr/n-GaN	5.5×10^{16}	5.2×10^{14}	3.01	0.36	0.39	0.34 ± 0.07
Gr/n-GaN	5.8×10^{17}	6.7×10^{14}	3.03	0.25	0.37	0.34 ± 0.04
Gr/n-GaN	6.0×10^{18}	7.8×10^{14}	3.07	0.10	0.32	0.33 ± 0.02

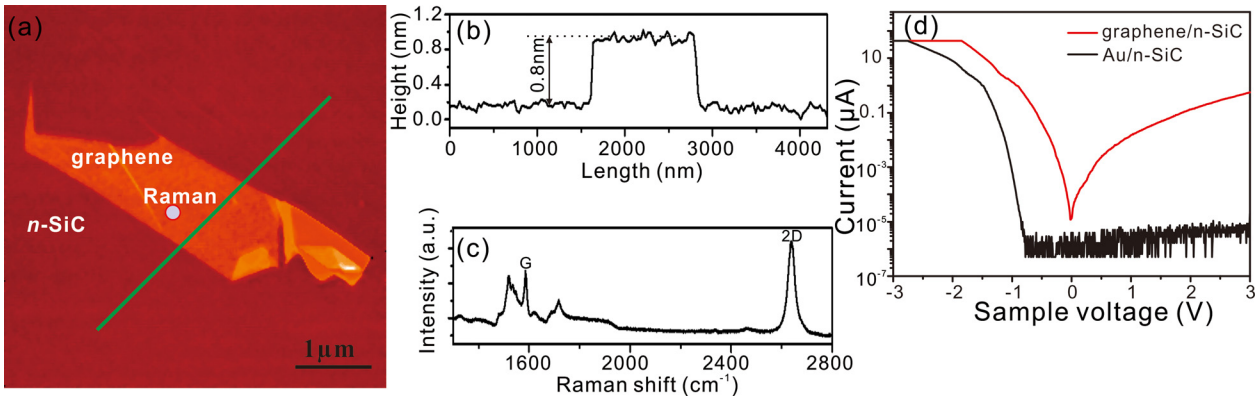

FIG. 8. The experimental results of the contact properties of graphene/n-SiC. (a) Tapping mode AFM image of an isolated single-layer graphene sheet on an n-SiC. (b) The height of the line profile plot acquired across the graphene/SiC boundary (green lines in (a)) showing approximately 0.8 nm. (c) The single layer graphene was confirmed by Raman spectra (632.8 nm laser wavelength) obtained from the corresponding spot in (a). a.u., arbitrary units. (d) Local I-V curves by Au coated tip were acquired from bare n-SiC (black dotted line) substrate and the graphene sheet (red dotted line), respectively.

between graphene and the semiconductor should account for the charge contributed by the interfacial states.

To validate the applicability of our model for other semiconductors, similar experimental and theoretical studies of the contacts between exfoliated graphene and n-type silicon carbide (n-SiC) with carrier density of $1.0\times10^{18}\,cm^{-3}$ were conducted. Fig. 8(a) shows the topography of an isolated single-layer graphene sheet on an n-SiC characterized by AFM. The AFM line profile across the graphene and the Raman spectrum as shown in Figs. 8(b) and 8(c) confirm the graphene to be a single layer sheet. Typical I-V curves for n-SiC are plotted in Fig. 8(d). The black symbol indicates the Au-coated AFM tip on n-SiC and the red symbol is for graphene. An obvious rectifying behavior similar to a Schottky barrier is observed. The barrier heights at graphene/n-SiC interfaces for experiments and calculation are 0.28 ± 0.02 V and 0.29 V, respectively, far lower than that of the contacts of Au/n-SiC with 0.67 V. The Fermi level in graphene goes up by 0.66 eV.

V. CONCLUSIONS

In conclusion, we have proposed a model for describing the transport mechanisms of graphene on semiconductors, by which the contact barrier heights and the Fermi level shift of the single-layer graphene can be calculated. Compared with experimental results, the interface separation and the relative dielectric constant in the interface gap can also be obtained approximately. The influences of the carrier density of semiconductors and the DOS of interfacial states were discussed intensively using experimental approaches and our theoretical model, which shows the dominate effects of interfacial states on the graphene/semiconductor contact properties. The theoretical and experimental results of graphene on the n-SiC surface provided more proof for our model. These approaches offer a deep insight into the physics of graphene/semiconductor contacts, which will also benefit recent topical research to incorporate graphene into various semiconductor devices.

ACKNOWLEDGMENTS

This work was supported by the Instrument Developing Project of the Chinese Academy of Sciences (Grant No. YZ200939), the National High Technology Research and Development Program of China (863 Program) (Grant No. 2011AA03A103), the Natural Science Foundation of China (Grant No. 11204347 and 11327804), the National Basic Research Program of China (Grant No. 2012CB619305), the Ministry of Science and Technology of China (Grant No. 2010DFA22770), and the Supercomputing Center, CNIC, CAS.

[1]F. Bonaccorso, Z. Sun, T. Hasan, and A. C. Ferrari, Nat. Photonics **4**, 611 (2010).
[2]C. Chen, M. Aykol, C. Chang, A. F. J. Levi, and S. B. Cronin, Nano Lett. **11**, 1863 (2011).
[3]S. Tongay, T. Schumann, X. Miao, B. R. Appleton, and A. F. Hebard, Carbon **49**, 2033 (2011).
[4]K. Chung, C. H. Lee, and G. C. Yi, Science **330**, 655 (2010).
[5]G. Jo *et al.*, Nanotechnology **21**, 175201 (2010).
[6]T. Sun, Z. L. Wang, Z. J. Shi, G. Z. Ran, W. J. Xu, Z. Y. Wang, Y. Z. Li, L. Dai, and G. G. Qin, Appl. Phys. Lett. **96**, 133301 (2010).
[7]S. Tongay, T. Schumann, and A. F. Hebard, Appl. Phys. Lett. **95**, 222103 (2009).

[8]X. M. Li *et al.*, Adv. Mater. **22**, 2743 (2010).
[9]K. Ihm *et al.*, Appl. Phys. Lett. **97**, 32113 (2010).
[10]Y. Gao, H. Yip, S. K. Hau, K. M. O'Malley, N. C. Cho, H. Chen, and A. K. Y. Jen, Appl. Phys. Lett. **97**, 203306 (2010).
[11]K. T. He, J. C. Koepke, S. Barraza-Lopez, and J. W. Lyding, Nano Lett. **10**, 3446 (2010).
[12]L. Magaud, F. Hiebel, F. Varchon, P. Mallet, and J. Y. Veuillen, Phys. Rev. B **79**, 161405 (2009).
[13]A. Mattausch and O. Pankratov, Phys. Rev. Lett. **99**, 76802 (2007).
[14]S. Y. Zhou, G. H. Gweon, A. V. Fedorov, P. N. First, W. A. De Heer, D. H. Lee, F. Guinea, A. Neto, and A. Lanzara, Nature Mater. **6**, 770 (2007).
[15]H. Zhong, Z. Liu, G. Xu, Y. Fan, J. Wang, X. Zhang, L. Liu, K. Xu, and H. Yang, Appl. Phys. Lett. **100**, 122108 (2012).
[16]W. Zhao, P. H. Tan, J. Liu, and A. C. Ferrari, J. Am. Chem. Soc. **133**, 5941 (2011).
[17]H. Hibino, H. Kageshima, M. Kotsugi, F. Maeda, F. Z. Guo, and Y. Watanabe, Phys. Rev. B **79**, 125437 (2009).
[18]A. H. Castro Neto, F. Guinea, N. Peres, K. S. Novoselov, and A. K. Geim, Rev. Mod. Phys. **81**, 109 (2009).
[19]G. Giovannetti, P. A. Khomyakov, G. Brocks, V. M. Karpan, J. van den Brink, and P. J. Kelly, Phys. Rev. Lett. **101**, 26803 (2008).
[20]S. M. Sze and K. K. Ng, *Physics of Semiconductor Devices*, 3rd ed. (Wiley, Hoboken, 2007).
[21]K. S. Kim *et al.*, Nature **457**, 706 (2009).
[22]K. S. Novoselov, D. Jiang, F. Schedin, T. J. Booth, V. V. Khotkevich, S. V. Morozov, and A. K. Geim, Proc. Natl. Acad. Sci. U.S.A. **102**, 10451 (2005).
[23]C. H. Lui, L. Liu, K. F. Mak, G. W. Flynn, and T. F. Heinz, Nature **462**, 339 (2009).
[24]A. C. Ferrari *et al.*, Phys. Rev. Lett. **97**, 187401 (2006).
[25]C. R. Dean *et al.*, Nat. Nanotechnol. **5**, 722 (2010).
[26]E. Lee, K. Balasubramanian, R. T. Weitz, M. Burghard, and K. Kern, Nat. Nanotechnol. **3**, 486 (2008).
[27]K. S. Novoselov, A. K. Geim, S. V. Morozov, D. Jiang, Y. Zhang, S. V. Dubonos, I. V. Grigorieva, and A. A. Firsov, Science **306**, 666 (2004).
[28]J. B. Pethica and W. C. Oliver, Phys. Scr. T **19A**, 61 (1987).
[29]R. Nowak, M. Pessa, M. Suganuma, M. Leszczynski, I. Grzegory, S. Porowski, and F. Yoshida, Appl. Phys. Lett. **75**, 2070 (1999).
[30]S. Chen, L. Liu, and T. Wang, Surf. Coat. Technol. **191**, 25 (2005).
[31]C. Oshima and A. Nagashima, J. Phys.: Condens. Matter **9**, 1 (1997).
[32]S. J. Sque, R. Jones, and P. R. Briddon, Phys. Status Solidi A **204**, 3078 (2007).